Delay-induced directional switches and mean switching time in swarming systems

Yongzheng Sun,[1] Wang Li,[1] Liang Li,[2,3,4,*] Guanghui Wen,[5,†] Sandro Azaele,[6,‡] and Wei Lin[7,8,9,§]

[1]*School of Mathematics, China University of Mining and Technology, Xuzhou 221116, China*
[2]*Department of Collective Behavior, Max Planck Institute of Animal Behavior, Konstanz 78464, Germany*
[3]*Centre for the Advanced Study of Collective Behavior, University of Konstanz, Konstanz 78464, Germany*
[4]*Department of Biology, University of Konstanz, Konstanz 78467, Germany*
[5]*School of Mathematics, Southeast University, Nanjing 210096, China*
[6]*Department of Physics and Astronomy "G. Galileo", University of Padova, Padova Via F. Marzolo 8, 35131, Italy*
[7]*Research Institute of Intelligent Complex Systems and MOE Frontiers Center for Brain Science, Fudan University, Shanghai 200433, China*
[8]*School of Mathematical Sciences, LMNS, and SCMS, Fudan University, Shanghai 200433, China*
[9]*Shanghai Artificial Intelligence Laboratory, Shanghai 200232, China*

(Received 27 December 2021; accepted 22 June 2022; published 18 July 2022)

Coordinated directional switches often emerge in moving biological groups replete with individual-level interactions. Recent self-propelled particles models can somewhat mimic the patterns of directional switches, but they usually do not include the effects of time delays in the interactions. Here, we focus on investigating the influence of time-delay interactions on the collective motion of swarming locusts, an experimentally well-studied system that exhibits ordered switches between clockwise and counterclockwise movement. We show, both analytically and numerically, that time delays of different types can affect the directional switches. Specifically, for the sufficiently small response delay, increasing the transmission delay can increase the mean switching time, while, for the large response delay, increasing the transmission delay may destroy the ordered directional switches. Our results decipher the role of time-delay interactions in the collective motion, which could be beneficial to the design of collective intelligent devices.

DOI: 10.1103/PhysRevResearch.4.033054

I. INTRODUCTION

Collective motions of coherence emergent in interacting multi-individual particles or swarming systems are omnipresent in nature and synthetic systems. Examples include foraging ant colonies [1,2], swarming locusts [3], schooling fish [4–7] or prawns [8], flocking birds [9], coordinated robots [10–12], and synchronized spacecrafts [13]. These emergent phenomena as well as the corresponding systems have attracted a great deal of attention from various research communities [14–24]. In the last decades, numerous theoretical [1,20,21,25,26] and empirical studies [3,4,17–19] have been carried out for exploring the underling mechanisms resulting in coordinated collective behaviors. Particularly in 1995, Vicsek and his colleagues proposed a simple self-propelled particles (SPP) model [26], where each moving individual is regarded as a particle orienting its velocity parallel to the average velocity of its local neighborhood particles. Extensive studies have been conducted on the Vicsek model and its variants for illustrating the phase transition between ordered and disordered states. The group density and the strength of noise have been found as the critical ingredients influencing the collective animal motion and the swarming phenomena of bacteria [18,24].

Most of the models focused majorly on how a large number of individuals move at almost the same velocities; however, those studies did not directly and systematically exploit an important and ubiquitous phenomenon that coherent animal groups can suddenly change in direction. Actually, directional switching behaviors can be often observed in biological systems, e.g., swarming bacteria [27], marching locusts [3], homing pigeons [28], starling flocks [29], and schooling fish [7] or prawns [8]. Some studies show that a switch in direction is a response to an external influence, such as the presence of a predator [7]. However, without the change in the external environment, the directional switches still occur, which has been confirmed by the experiments on various densities of desert locusts [3], glass prawns [8], and pigeons [28].

The initial studies of directional switching behavior focused on how the densities affect collective alignment of animal groups. Evidences emerging from both experimental and theoretical studies suggested that disordered animal groups can transit to ordered motion as the group density increases [3]. Recently, more complex situations with randomness have been taken into account, which demonstrated the positive role of intrinsic noise in enhancing the ordered switches in direction [1,7,30,31]. It was shown that directional switches of moving locusts are produced as a consequence of the ergodic

*lli@ab.mpg.de
†ghwen@seu.edu.cn
‡S.Azaele@unipd.it
§wlin@fudan.edu.cn

Published by the American Physical Society under the terms of the Creative Commons Attribution 4.0 International license. Further distribution of this work must maintain attribution to the author(s) and the published article's title, journal citation, and DOI.

random evolution of the system [30]. Although the existing models could somewhat mimic the ordered directional switching behaviors, they only considered the instantaneous interactions but often omitted the influence of the time-delay interactions that arise in many collective motions due to finite communication speeds and information-processing times [32,33]. Since time delays play important roles in inducing the emergence of swarms of living organisms [32], an introduction of their influence into the model could be beneficial to deciphering the essential underlying mechanism that produces the phase transition process of real animal groups.

The animal group movement usually involves two types of time delays, viz., the transmission delay and the response delay [34–36]. The transmission delay corresponds to the amount of the time required for an individual to receive information from its neighbors, while the response delay (also known as the information processing delay) to the amount of the time required for an individual to process the received information and adjust its state. In addition, the mean switching time (MST) between different moving directions is an important indicator, describing the ordered extent of moving groups. Our previous investigation [33] only numerically reported an elementary result that increasing the transmission delay may significantly increase the MST of directional switches; however, it considers neither the interplay between the two types of time delays nor how this interplay contributes to the directional switches by estimating the MST. Therefore, this article intends to investigate all these time-delay interactions on the directional switches in the locust nymphs that are supposed to move in an experimental arena of ring shape.

This article is organized as follows. We start with a time-delay model that includes either the information processing delay or the transmission delay. Then, we investigate a generalized model which contains both types of delays. Indeed, we propose a general mathematical framework to calculate the MST for moving groups with delayed interactions. Treating the MST as a function of the group density and the time delay, we show that the MST monotonically increases with the the group density or/and the transmission delay, but decreases with the response delay. Particularly in those delayed-coupled individuals, both the response and the transmission delays are responsible for the ordered directional switches, in contrast to the previous studies [1,3,30,31] where only noise and group density can induce switches in moving directions. Finally, we close this article by providing some discussion and perspective remarks.

II. RESULTS

A. MST for individual-based systems with response delays

In a real biological experiment, locust nymphs of various densities were put in a homogeneous ring-shaped experimental arena [3]. It was found that the groups of locust nymphs with high density, instead of marching randomly between the two directions, marched in one direction for several hours. After a period of time, they suddenly turned their directions in only a few minutes and marched in an opposite direction for a number of hours. According to the ring-shaped experimental arena, we assume that, in our model, N individuals move along a circle, which is denoted by the interval $\Omega = [0, 1)$ with a periodic boundary condition. The state of each individual is described by its position, denoted by $X_i \equiv X_i(t) \in \Omega$, and by its velocity, $V_i \equiv V_i(t)$ for $i = 1, 2, \cdots, N$. Denote by $J_{i,R}(t) = \{j \in \{1, \cdots, N\} \mid \min(d_{ij}, 1 - d_{ij}) \leqslant R\}$ the set of the ith individual's neighbors at time t, where $d_{ij} = |X_i - X_j|$. Thus, each individual adjusts its state based on the behaviors of its neighbors in the set $J_{i,R}(t)$.

In Vicsek's model [26] and its variants [3,31] as well, the interactions among individuals are assumed to occur instantaneously. Here, we introduce the effect of time-delayed interactions. First, for simplicity, the information transmission is supposed to be instantaneous while the response delay $\tau > 0$, corresponding to processing, cognitive, or execution time, is taken into account. Then, we have the following time-delayed system:

$$dX_i = V_i(t)\,dt, \tag{1}$$

$$dV_i = [\mathrm{sign}(U_{i,R}(t-\tau)) - V_i(t-\tau)]dt + \eta\,dW_i, \tag{2}$$

where each dW_i is the standard white noise (independently sampled for each individual), $\eta > 0$ represents the strength of noise, $\mathrm{sign}(\cdot) : \mathbb{R} \to \{-1, 0, 1\}$ is the signum function, and

$$U_{i,R}(t) = \frac{1}{|J_{i,R}(t)|} \sum_{j \in J_{i,R}(t)} V_j(t) \tag{3}$$

is the mean of the velocity at time t of the individuals in the set $J_{i,R}(t)$. Also, we denote by $U(t)$ the average velocity of the whole group. As such, $U(t) \equiv U_{i,R}(t)$ for R larger than 0.5 and arbitrary i. Additionally, it is supposed that each individual needs time τ to adjust its velocity when the velocities of its neighbors are received, so the ith individual in Eq. (2) of the time-delayed model updates its velocity at time t according to the information of the neighbored individuals' velocities at time $t - \tau$. Clearly, as $\tau = 0$, the model of Eqs. (1)–(3) is equivalent to the standard Vicsek's SPP model [3,31].

Through simulating the system of Eqs. (1)–(3) for different N, we investigate the influence of the group density on the collective motion. All the stochastic differential equations are solved using the standard Euler-Maruyama numerical scheme [37] with a time step $\triangle t = 0.01$. The initial positions of the individuals are taken uniformly from the interval [0,1], and the initial velocities are normally distributed with zero mean and unit variance. The parameter of the interaction range is used as $R = 0.1$, which corresponds to 27.8 cm interaction range of the locusts in a ring-shaped experimental arena [3]. And the results are similar if the other values of R are taken into account. The typical evolutions of the average velocity U of the whole group are shown in Fig. 1(a), where, without any change in the external environment, the group switches suddenly its velocity in an opposite direction [i.e., from left ($U(t) < 0$) to right ($U(t) > 0$) or from right to left]. Indeed, the group with a low density switches its direction more frequently than the group with a high density. We numerically estimate the MST between the switches from long-term stochastic simulations. As significantly shown in Fig. 1(b), the MST increases monotonically with the group size. This implies that, in spite of the presence of delayed interaction, the disordered movement of individuals within the group can transit to the highly aligned collective motion as the group

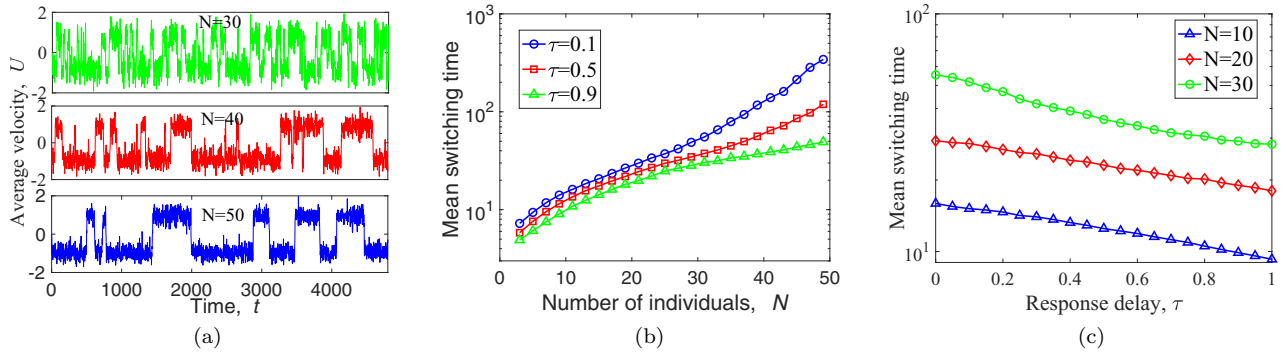

FIG. 1. Effects of the group density and the response delay, respectively, on the collective behaviors of the model of Eqs. (1)–(3). (a) The average velocity $U(t)$ changes with time evolution for the model with $\tau = 0.1$, $\eta = 2$, $R = 0.1$, and different $N = 30$ (green), 40 (red), and 50 (blue). Here and throughout, the initial positions of individuals are taken uniformly from the interval [0,1], the initial velocities are set as the numbers normally distributed with zero mean and unit variance, and the time step is selected as $\triangle t = 0.01$ for $t \in [0, 10^6]$. (b) The MST as a function of the group size N, for different τ. (c) The MST as a function of the response delay τ, for $\eta = 2$, $R = 0.1$, and different N.

size N increases. This is akin to the phenomena observed in the experiments [3] and to the results obtained in the classical Vicsek's model and its variants that are free of time delays [3,26,31].

Now, we study how the response delay influences the group motion. Still in Fig. 1(b), we can see that, for any fixed N, the MST of the group with smaller response delay is longer than that of the group with larger response delay. Obviously, the frequency of directional switches increases monotonically with the response delay. This is further confirmed from another viewpoint [see Fig. 1(c)]. Here, the MST decreases as the response delay increases. *Therefore, increasing the response delay can induce dramatically directional switches in the collective swarming motion.*

In order to quantify how the interplay between the group density and the response delay contributes to the switches emergent, we study the collective behavior of a mean-field model. As such, suppose all the individuals to be interacting with each other, and use the global velocity average $U(t)$ to replace $U_{i,R}(t)$ in Eq. (2). Then, we get

$$dV_i = [\mathrm{sign}(U(t-\tau)) - V_i(t-\tau)]dt + \eta\, dW_i. \tag{4}$$

Taking the average of all these equations for $i = 1, \cdots, N$ yields an Itô's stochastic differential equation for $U(t)$ as

$$dU = [\mathrm{sign}(U(t-\tau)) - U(t-\tau)]dt + \eta N^{-1/2}\, dW. \tag{5}$$

Denote by $P(u,t)$ the probability density of the stochastic process defined by Eq. (5). Then, $P(u,t)du$ stands for the probability of the global velocity average $U(t) \in [u, u+du)$, satisfying the following delayed Fokker-Planck equation (as the one developed in Ref. [38]):

$$\frac{\partial}{\partial t}P(u,t) = -\frac{\partial}{\partial u}\int_{\mathbb{R}}[\mathrm{sign}(u_\tau) - u_\tau]P(u,t;u_\tau,t-\tau)du_\tau + \frac{\eta^2}{2N}\int_{\mathbb{R}}\frac{\partial^2}{\partial u^2}P(u,t;u_\tau,t-\tau)du_\tau, \tag{6}$$

where $u_\tau = u(t-\tau)$ and $P(u,t;u_\tau,t-\tau)$ is the joint probability density of $U(t)$. Denote by $P_{\mathrm{st}}(u)$ the stationary probability distribution (SPD) of $U(t)$, and by $P_{\mathrm{st}}^{(1)}(u)$ the first-order approximation of the SPD. Using the small delay approximation method [38], we obtain the first-order approximation to $P_{\mathrm{st}}(u)$ as

$$P_{\mathrm{st}}^{(1)}(u) = \frac{1}{Z}\exp\big(-\phi(u)\big), \tag{7}$$

where Z is a normalization constant and the potential $\phi(u)$ is given by $\phi(u) = -2NV_{\mathrm{eff}}(u)/\eta^2$ and the function V_{eff} is given by

$$V_{\mathrm{eff}}(u) = \sqrt{\frac{N}{2\pi\eta^2\tau}}\int_0^u du'\int_{-\infty}^{\infty}du_\tau[\mathrm{sign}(u_\tau) - u_\tau] \times \exp\left(-\frac{[u_\tau - u' - (\mathrm{sign}(u') - u')\tau]^2}{2\eta^2\tau/N}\right). \tag{8}$$

Through further detailed calculations (refer to Methods), $V_{\mathrm{eff}}(u)$ in (8) becomes

$$\begin{aligned} V_{\mathrm{eff}}(u) &= \int_0^u \mathrm{erf}\left(\frac{\psi(u')}{\sqrt{2\eta^2\tau/N}}\right)du' - \tau|u| - (1-\tau)\frac{u^2}{2} \\ &= \int_0^u \mathrm{erf}\left(\sqrt{\frac{N}{2\eta^2\tau}}[(1-\tau)v + \tau\,\mathrm{sign}(v)]\right)dv \\ &\quad -\tau|u| - (1-\tau)\frac{u^2}{2}. \end{aligned} \tag{9}$$

For the case $N \gg 1$ and $0 \leqslant \tau < 1$, using the asymptotic expansion of the function $\mathrm{erf}(\cdot)$ yields:

$$\int_0^u \mathrm{erf}\left(\frac{\psi(u')}{\sqrt{2\eta^2\tau/N}}\right)du' \approx |u|$$

and

$$V_{\mathrm{eff}}(u) \approx (1-\tau)\left(|u| - \frac{u^2}{2}\right). \tag{10}$$

Hence, from (7), the first-order approximation of $P_{\mathrm{st}}^{(1)}(u)$ becomes

$$P_{\mathrm{st}}^{(1)}(u) = \frac{k_\tau e^{2k_\tau^2(|u|-u^2/2)}}{e^{k_\tau^2}\sqrt{\pi}(1+\mathrm{erf}(k_\tau))}, \tag{11}$$

where $k_\tau = \sqrt{N(1-\tau)}/\eta$. It is easy to see from Fig. 2 that $P_{\mathrm{st}}^{(1)}(u)$ has two global maxima at $u = \pm 1$. For $N \gg 1$ and

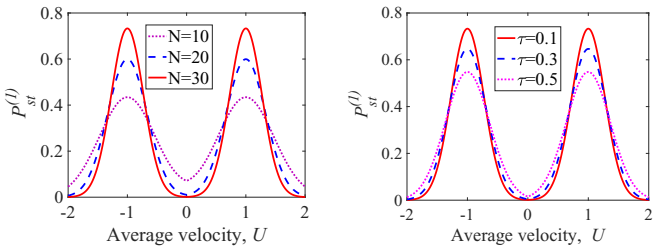

(a) (b)

FIG. 2. The first-order approximation $P_{\rm st}^{(1)}$, obtained in (11) for $P_{\rm st}$, changes with the average velocity U, for system (5) with $R = 0.5$ and $\eta = 2$. Here, $\tau = 0.1$ is fixed but N is differently selected (a), and $N = 30$ is fixed but τ is differently selected (b).

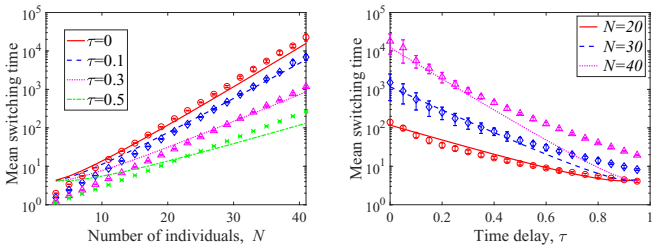

(a) (b)

FIG. 3. The MST obtained using Eqs. (16)–(17) (lines in different types) versus the MST obtained using the stochastic simulations (symbols in different types). (a) The MST as a function of the group density N, respectively, for different delays $\tau = 0$ (solid line, circles), $\tau = 0.1$ (dashed line, diamonds), $\tau = 0.3$ (dotted line, triangles), and $\tau = 0.5$ (dash-dotted line, crosses). (b) The MST as a function of the response delay τ, respectively, for $N = 20$ (solid line, circles), $N = 30$ (dashed line, diamonds), and $N = 40$ (dash-dotted line, triangles).

$0 < \tau < 1$, $\mathrm{erf}(k_\tau) \approx 1$, so that, from (11), we have

$$P_{\rm st}^{(1)}(u = \pm 1) \approx \frac{k_\tau}{2\sqrt{\pi}} = \frac{\sqrt{N(1-\tau)}}{2\eta\sqrt{\pi}}.$$

This implies that one can clearly distinguish the quasistationary states when the group size N becomes large or the response delay τ becomes sufficiently small. This is also consistent with the results shown in Fig. 1.

Now, we are to calculate the *mean first passage time* for system (5), denoted by $T(-1 \to +1) = T(+1 \to -1) = T(u)$, i.e., the average time cost for the particle jumping from one well of the effective potential to the other, for small τ. As such, we introduce the stochastic differential equation without delay as follows:

$$dU = -\zeta'(u)dt + \sqrt{2\epsilon_\tau}dW, \tag{12}$$

where $\zeta(u) = u^2/2 - |u|$ is the effective potential and $\epsilon_\tau = \eta^2/2N(1-\tau)$ with $0 \leqslant \tau < 1$. A direct calculation yields the SPD for (12) as

$$P_{\rm st}^{(\rm proc)}(u) = Ze^{-\zeta(u)/\epsilon_\tau}. \tag{13}$$

It is easy to see from (11) and (13) that the time-delayed system (5) and the nondelayed system (12) share the same SPD of the average velocity $U(t)$. Thus, systems (5) and (12) own the same mean first passage time from one steady state $u = 1$ to the other $u = -1$. Moreover, the response delay τ is also shown in the diffusion parameter of ϵ_τ, which allows us to analyze the influence of the response delay on the directional switches. Therefore, system (5) can be well approximated by the non-delayed system (12). Here, we assume that the dynamics are governed by (12). If a particle is initially located at $u \neq 0$ (i.e., $P\{u(0) \neq 0\} = 1$) in one of the wells, then $T(u)$, the mean first passage time of the particle jumping into the other well, satisfies (see [39], p. 132)

$$\epsilon_\tau T''(u) - \zeta'(u)T'(u) = -1, \tag{14}$$

where the boundary conditions (absorbing at zero and reflecting at $+\infty$) satisfy $T(0) = 0$ and $\lim_{u\to+\infty} T'(u) = 0$, because we assume that a particle starts off from the right well near the minimum at $u = 1$. Correspondingly, the solution is

$$T(u) = \frac{1}{\epsilon_\tau}\int_0^u e^{\frac{\zeta(y)}{\epsilon_\tau}}\int_y^\infty e^{-\frac{\zeta(z)}{\epsilon_\tau}}dydz. \tag{15}$$

Since we are interested in the regime of small fluctuations (i.e., $\epsilon_\tau \to 0$), for any u close to the minimum, $T(u)$ in (15) is well approximated by

$$T(N,\tau) \simeq \sqrt{\frac{\pi\eta^2}{N(1-\tau)}}\exp\left(\frac{N}{\eta^2}(1-\tau)\right). \tag{16}$$

Clearly, the mean fist passage time is equivalent to the MST between different moving directions. The approximation obtained in (16) implies that the MST is an increasing function with respect to the group density but it decreases monotonically with the response delay.

In particular, for $\tau = 0$, the MST in (16) for the SPP model (4) degenerates as

$$T_N = \sqrt{\frac{\pi\eta^2}{N}}\exp\left(\frac{N}{\eta^2}\right), \tag{17}$$

which is the MST (see Methods) for the following SPP model without delay interactions,

$$dV_i = [\mathrm{sign}(U(t)) - V_i(t)]dt + \eta\, dW_i. \tag{18}$$

Comparing these two MSTs obtained, respectively, in (16) and in (17), we see that the existence of the response delay can significantly decrease the MST, which means that the response delay can induce the directional switches of moving groups. In addition, the MST for the SPP model with or without delay is an increasing function of the group density, which implies that group density is a crucial factor for the spontaneously directional switches.

From Fig. 3, which compares the MSTs, respectively, derived from the simulation and calculated from the analytical estimation in (16), we see that the analytical estimation matches the simulations well for sufficiently small τ and large N. Both theoretical and numerical results show that swarming groups with higher densities and smaller response delays have relatively lower frequencies of directional switches. This further indicates that improving the information process speed (i.e., decreasing the response delay of a moving group) can increase its MST of the directional switches.

B. MST for systems with transmission delays

Apart from the response delay introduced in the model of (1)–(2), the transmission delay can not be neglected, because it arises from a realistic situation where moving individuals need time to receive the state information from their neighbors. Thus, we consider the following model

$$dV_i = \left[\text{sign}\left(U_i^R(t-\omega)\right) - V_i(t)\right]dt + \eta\, dW_i. \quad (19)$$

Here, $\omega > 0$ is the transmission delay, indicating that each individual needs time ω to receive the velocity information of its neighbors and the adjustment time is not taken into consideration. Thus, the ith individual updates its velocity according to the combination of its own velocity at time t and the mean velocity of its neighbors at time $t-\omega$. The other parameters are the same as those set for system (2).

When the interaction radius is sufficiently large, system (19) is reduced as

$$dV_i = [\text{sign}(U(t-\omega)) - V_i(t)]dt + \eta\, dW_i. \quad (20)$$

Similarly, the average velocity $U(t)$ of the whole group satisfies the system,

$$dU = [\text{sign}(U(t-\omega)) - U(t)]dt + \eta N^{-1/2}\, dW. \quad (21)$$

Thus, $P(u,t)$, the probability distribution function for the variable U produced by system (21), satisfies the following Fokker-Planck equation (refer to Ref. [38]):

$$\frac{\partial}{\partial t}P(u,t) = -\frac{\partial}{\partial u}\int_{\mathbb{R}}[\text{sign}(u_\tau) - u]P(u,t;u_\tau,t-\tau)du_\tau + \frac{\eta^2}{2N}\int_{\mathbb{R}}\frac{\partial^2}{\partial u^2}P(u,t;u_\tau,t-\tau)du_\tau. \quad (22)$$

Still using the small delay approximation method [38], we obtain the first-order approximation of the SPD as

$$P_{\text{st}}^*(u) \approx D\exp\big(-\xi(u)\big), \quad (23)$$

where D is a normalization constant and the potential $\xi(u)$ fulfills

$$\xi(u) = -\frac{2N}{\eta^2}\left\{\int_0^u \text{erf}\left(\sqrt{\frac{N}{2\eta^2\omega}}[(1-\omega)v + \omega\cdot\text{sign}(v)]\right)dv - \frac{u^2}{2}\right\}. \quad (24)$$

The approximation of the SPD specified in (23) has two global maxima at $u = \pm 1$, as shown in Fig. 4. In Fig. 4(a), it is easy to distinguish the quasistationary states as the group size becomes large. This indicates that, as the group density increases, the turning rate of the group significantly decreases. In Fig. 4(b), the group with a larger ω has a smaller potential function. Hence, increasing the transmission delay can also significantly increase the MST of the directional switches. Furthermore, suppose a particle to start off from the left well near the minimum $u = -1$ for a sufficiently small ω. Then, the MST as a function of N and ω is calculated as (see Ref. [39]):

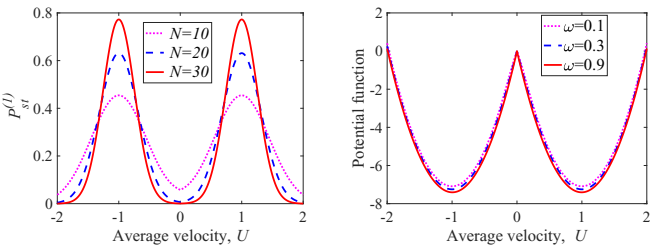

(a) (b)

FIG. 4. (a) The first order approximation $P_{\text{st}}^{(1)}$, obtained in Eq. (11), changes with the average velocity U for delay $\omega = 0.1$ and different population size N. (b) The potential function as a function of U for $N = 30$ and different delay ω. Here, system (21) with $R = 0.5$ and $\eta = 2$ is taken into account.

$$T(N,\omega) = \frac{2N}{\eta^2}\int_{-1}^0 \frac{1}{P_{\text{st}}^*(u)}\int_{-\infty}^u P_{\text{st}}^*(s)dsdu = \frac{2N}{\eta^2}\int_{-1}^0 \exp(\xi(u))\int_{-\infty}^u \exp(-\xi(s))dsdu. \quad (25)$$

Based on the analytical result obtained in Eq. (25), we calculated the MST for $\omega = 0.1$ and for different N in Fig. 5. We also compare the this calculated result with the MST obtained directly from the stochastic simulations, which shows them in a high consensus for larger values of N.

C. Individual-based system with both response and transmission delays

Here, we are to investigate the effect of both the response and the transmission delays on the MST. As such, we incorporate the transmission delay into system (2), which yields a generalized model:

$$dV_i = \left[\text{sign}\left(U_i^R(t-\tau-\omega)\right) - V_i(t-\tau)\right]dt + \eta\, dW_i, \quad (26)$$

where the parameters are the same as those in system (2). To be candid, system (26) with both the response and the

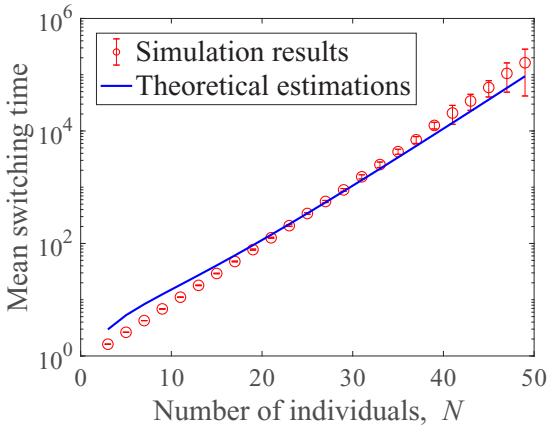

FIG. 5. The MST as a function of the group density. Here, for $\omega = 0.1$, the solid line is depicted using Eq. (25), while the circles are depicted using the stochastic simulations.

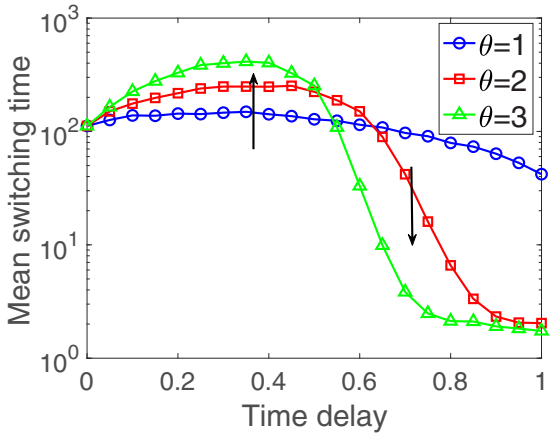

FIG. 6. The MST as a function of the response delay τ for the system (26) with $N = 30$, $\eta = 2$, and $R = 0.1$, particularly as the transmission delay $\omega = \theta\tau$ for $\theta = 1, 2, 3$. Here, each arrow indicates the changing direction of the MST with increasing θ and for the given response delay τ.

transmission delays does not admit a feasible analytical treatment, even though, from the above analyses, we have obtained the estimation of the MST for the model with either the response delay or the transmission delay. So, we calculate the MST from the long-term stochastic simulations. In Fig. 6, we set $\omega = \theta\tau$ with $\tau \in [0, 1]$ and $\theta = 1, 2, 3$. For each pair (τ, ω), we performed the stochastic simulations for the system (26) and calculated the MST correspondingly. It can be seen from Fig. 6 that increasing the transmission delay can inhibit the directional switching of swarming locusts as the response delay is sufficient small; however, it may induce frequently directional switches when the response delays are sufficiently large. Thus, the groups with small response delay and large transmission delay likely have directional switches of low frequency. In those previous studies [30,31], it was shown that noise can play a crucial role in the directional switches of swarming locusts. The results in Fig. 6 reveal that, in addition to the noise, the time delays aroused by the limited information transmission and the processing speed also have important influence on the directional switching behavior of the collective motion.

III. CONCLUDING REMARKS

To summarize, in this article, we studied the directional switching behaviors of the collective motion, quantifying the influence of the group density, the response delay, and the information transmission delay on the MST between two moving directions. Particularly, we first generalized the standard Vicsek model to a computational framework with the local alignment interactions and the response delay, in which individuals only receive the information from its neighbors and require some time to adjust their velocities. For this generalized model, we numerically investigated the influence of the factors, including the group size and the response delay, on the MST. To get deep insights into the mechanism behind the influence of the factors, we studied the collective dynamics of the mean-field model with the global interactions. As a result, we obtained the analytical estimation of the MST with respect to the group size and the response delay. Also, we considered the model with the information transmission delay and calculated its MST by assuming the interaction radius is sufficiently large. Moreover, we also numerically investigated the model with both the response and the transmission delays.

We have articulated a framework for calculating the MST of the stochastic time-delay systems, where the analytical results match the corresponding numerical results fairly well. More precisely, we find that, as the density of the group increases, a rapid transition occurs from a disordered movement of the individuals within the group to a highly aligned collective motion. We also find that the response delay can induce the directional switches because the MST is a decreasing function of the response delay. By simulating the system simultaneously with the response and the transmission delays, we further find that, for the case of smaller response delay, increasing the transmission delays may significantly reduce the turning rate of moving directions, while, for the case of larger response time delay, increasing the transmission delay may result in high frequency directional switching. Our results show that, apart from the noise and the group densities, the time-delay interactions also play important roles in inducing the directional switches of the moving animal groups. This complements the results in the literature where the time delays were not taken into account in the modeling.

To be candid, all individuals in our models are all supposed to be moving along a one-dimensional circle, so the obtained results are not applicable directly to illustrating the collective motions in two or three-dimensional spaces. Recent progress has showed that the phase transition of collective dynamics in the spaces of higher dimensions are remarkably different [17]. In order to improve our understanding phase transition of moving animal groups, directional switches of collective motions in these spaces of different dimensions are included in our present or/and future research topics. Moreover, the time delays for the realistic moving animals are not necessarily the same but often randomly distributed in some specific range. Thus, highly anticipated is a novel extension of the method currently used in this article to a more technical and advanced version that can treat the moving individuals possessing randomly distributed delays. Additionally, the network topologies of the realistic moving animal groups are not necessarily time-invariant but often temporally changing [40,41]. Thus, detecting the time-varying topologies by the methods developed in [42–44] and further extending the method used in this article to the case where the moving groups possess time-varying topologies could be some of our future research topics.

Moreover, in this article, we always assume that each individual adjusts its velocity to the average velocity of individuals in its local neighborhood. However, this configuration does not include the social interaction, an important factor influencing the moving group. In fact, the social interaction implies that individual tends to align its status with that of individual which has strong social ties, but that might be separated by a relatively long Euclidean distance [21,45]. This kind of interactions can be described by the social networks which has been observed in the moving pigeons [28] and in the schooling fish as well [46,47]. The phase transition of

moving locusts on adaptive networks with random topologies has been discussed in [48], where each node represents an insect, and the links represent the interactions between locusts. Thus, further extending the method used in this article to the case where the moving groups possess social interactions could also be some of our future research topics.

The data sets generated during and/or analyzed during the current study are all available from the corresponding authors upon request.

All relevant computer codes are available from the authors upon request.

ACKNOWLEDGMENTS

This work was supported by the National Natural Science Foundation of China (Grants No. 1161101243, No. 11925103, No. 22120102001, No. 62073079) and Natural Science Foundation of Jiangsu (Grant No. BK20211241). This work was also supported by the STCSM (No. 19511132000, No. 19511101404, and No. 2021SHZDZX0103). L.L. acknowledges the Deutsche Forschungsgemeinschaft (DFG, German Research Foundation) under Germany's Excellence Strategy–EXC 2117-422037984, the Max Planck Society, and great support from Couzin's Lab.

Y.S., W.Li, G.W., S.A., and W.Lin conceived the project. Y.S., S.A. and W.Lin analyzed the model. Y.S., W.Li, L.L., and W. Lin performed the experiments. All authors analyzed the data. W.Lin wrote the paper with help from S.A. and Y.S.

APPENDIX: METHODS

1. Potential function

In the main text we have defined V_{eff} of the potential function $\phi(u)$. Let

$$V_{\text{eff}}(u) = \sqrt{\frac{N}{2\pi\eta^2\tau}} \int^{u} h_{\text{eff}}(u')du' \tag{A1}$$

with

$$\begin{aligned} h_{\text{eff}}(u') &= \int_{-\infty}^{\infty} [\text{sign}(u_\tau) - u_\tau] \exp\left(-\frac{[u_\tau - \psi(u')]^2}{2\eta^2\tau/N}\right) du_\tau \\ &= \int_{-\infty}^{\infty} \text{sign}(u_\tau) \exp\left(-\frac{[u_\tau - \psi(u')]^2}{2\eta^2\tau/N}\right) du_\tau \\ &\quad - \int_{-\infty}^{\infty} u_\tau \exp\left(-\frac{[u_\tau - \psi(u')]^2}{2\eta^2\tau/N}\right) du_\tau \\ &\triangleq I_2 - I_1 \end{aligned} \tag{A2}$$

and $\psi(u') = (1-\tau)u' + \tau\,\text{sign}(u')$. Further letting $\mu = u_\tau - \psi(u')$ and $\nu = \frac{\mu}{\sqrt{2\eta^2\tau/N}}$, we obtain

$$\begin{aligned} I_1 &= \int_{-\infty}^{\infty} \mu \exp\left(-\frac{\mu^2}{2\eta^2\tau/N}\right) d\mu \\ &\quad + \psi(u') \int_{-\infty}^{\infty} \exp\left(-\frac{\mu^2}{2\eta^2\tau/N}\right) d\mu \\ &= \psi(u') \int_{-\infty}^{\infty} \exp\left(-\frac{\mu^2}{2\eta^2\tau/N}\right) d\mu \\ &= \psi(u')\sqrt{2\eta^2\tau/N} \int_{-\infty}^{\infty} \exp(-\nu^2) d\nu \\ &= \psi(u')\sqrt{2\pi\eta^2\tau/N}, \end{aligned} \tag{A3}$$

where the validity of the last equality follows from the fact that $\int_{-\infty}^{\infty} \exp(-u^2)du = \sqrt{\pi}$. For I_2, we calculate as follows:

$$\begin{aligned} I_2 &= \int_{-\infty}^{\infty} \text{sign}(u_\tau) \times \exp\left(-\frac{[u_\tau - \psi(u')]^2}{2\eta^2\tau/N}\right) du_\tau \\ &= -\int_{-\infty}^{0} \exp\left(-\frac{[u_\tau - \psi(u')]^2}{2\eta^2\tau/N}\right) du_\tau \\ &\quad + \int_{0}^{\infty} \exp\left(-\frac{[u_\tau - \psi(u')]^2}{2\eta^2\tau/N}\right) du_\tau \\ &\triangleq I_3 + I_4. \end{aligned}$$

Again, letting $\mu = u_\tau - \psi(u')$ and $\nu = \frac{\mu}{\sqrt{2\eta^2\tau/N}}$ yields, respectively:

$$\begin{aligned} I_3 &= -\int_{-\infty}^{-\psi(u')} \exp\left(-\frac{\mu^2}{2\eta^2\tau/N}\right) d\mu \\ &= -\int_{-\infty}^{0} \exp\left(-\frac{\mu^2}{2\eta^2\tau/N}\right) d\mu \\ &\quad - \int_{0}^{-\psi(u')} \exp\left(-\frac{\mu^2}{2\eta^2\tau/N}\right) d\mu \\ &= -\sqrt{2\eta^2\tau/N}\left[\int_{-\infty}^{0} \exp\left(-\nu^2\right) d\nu \right. \\ &\quad \left. + \int_{0}^{\frac{-\psi(u')}{\sqrt{2\eta^2\tau/N}}} \exp(-\nu^2) d\nu\right] \end{aligned}$$

and

$$\begin{aligned} I_4 &= \int_{-\psi(u')}^{\infty} \exp\left(-\frac{\mu^2}{2\eta^2\tau/N}\right) d\mu \\ &= \sqrt{2\eta^2\tau/N} \int_{\frac{-\psi(u')}{\sqrt{2\eta^2\tau/N}}}^{\infty} \exp(-\nu^2) d\nu \\ &= \sqrt{2\eta^2\tau/N}\left[\int_{\frac{-\psi(u')}{\sqrt{2\eta^2\tau/N}}}^{0} \exp(-\nu^2) d\nu + \int_{0}^{\infty} \exp(-\nu^2) d\nu\right]. \end{aligned} \tag{A4}$$

Thus, we have

$$\begin{aligned} I_3 + I_4 &= -\sqrt{2\eta^2\tau/N}\left[\int_{0}^{\frac{-\psi(u')}{\sqrt{2\eta^2\tau/N}}} \exp(-\nu^2) d\nu \right. \\ &\quad \left. - \int_{\frac{-\psi(u')}{\sqrt{2\eta^2\tau/N}}}^{0} \exp(-\nu^2) d\nu\right] \\ &= \sqrt{2\eta^2\tau/N}\left[\int_{0}^{\frac{\psi(u')}{\sqrt{2\eta^2\tau/N}}} \exp(-\omega^2) d\omega\right. \end{aligned}$$

$$+\int_{\frac{-\psi(u')}{\sqrt{2\eta^2\tau/N}}}^{0}\exp(-v^2)dv\Bigg]$$
$$=\sqrt{2\eta^2\tau/N}\int_{\frac{-\psi(u')}{\sqrt{2\eta^2\tau/N}}}^{\frac{\psi(u')}{\sqrt{2\eta^2\tau/N}}}\exp(-v^2)dv$$
$$=2\sqrt{2\eta^2\tau/N}\int_{0}^{\frac{\psi(u')}{\sqrt{2\eta^2\tau/N}}}\exp(-v^2)dv$$
$$=\sqrt{2\pi\eta^2\tau/N}\cdot\mathrm{erf}\left(\frac{\psi(u')}{\sqrt{2\eta^2\tau/N}}\right), \tag{A5}$$

where $\omega=-v$ and $\mathrm{erf}(u)=\frac{2}{\sqrt{\pi}}\int_0^u e^{-t^2}dt$. Consequently, together with (A2), (A3), and (A5), it follows that

$$h_{\mathrm{eff}}(u')=\sqrt{\frac{2\pi\eta^2\tau}{N}}\left[\mathrm{erf}\left(\frac{\psi(u')}{\sqrt{2\eta^2\tau/N}}\right)-\psi(u')\right]. \tag{A6}$$

Substituting Eq. (A6) into Eq. (A1) yields Eq. (9). This makes it possible to obtain the potential function in the main text.

2. MST estimation for SPP model without delay

To calculate the MST for the SPP model without delay, we investigate the following Itô stochastic differential equation for $U(t)$ from system (18):

$$dU=[\mathrm{sign}(U(t))-U(t)]dt+\eta N^{-1/2}dW. \tag{A7}$$

Denote by $P(u,t)$ the probability distribution of the group velocity average $U(t)$. It satisfies the following Fokker-Planck equation:

$$\frac{\partial}{\partial t}P(u,t)=-\frac{\partial}{\partial u}[\mathrm{sign}(u)-u]P(u,t)+\frac{\eta^2}{2N}\frac{\partial^2}{\partial u^2}P(u,t).$$

The SPD for system (A7) is obtained as

$$P_{\mathrm{st}}(u)=C\exp\left(\int_0^u\frac{2N^2}{\eta}[\mathrm{sign}(u)-u]du\right)$$
$$=C\exp\left(-\frac{2N^2}{\eta}\zeta(u)\right),$$

where C is a normalization constant. Furthermore, assume that a particle starts off from the left well near the minimum at $u=-1$. Then, the corresponding mean first passage time satisfies the following equation (see [39]):

$$[\mathrm{sign}(u)-u]\cdot\frac{dT}{du}+\frac{\eta^2}{2N}\frac{d^2T}{du^2}=-1, \tag{A8}$$

which can be further analytically calculated as

$$T_N=\frac{2N^2}{\eta}\int_{-1}^{0}\exp\left(\frac{2N^2}{\eta}\zeta(u)\right)$$
$$\times\int_{-\infty}^{s}\exp\left(-\frac{2N^2}{\eta}\zeta(u)\right)dsdu.$$

Here, the boundary conditions $T(0)=0$ and $T'(-\infty)=0$ are used. Clearly, T_N as obtained above is a function of N. Using the Taylor expression of function $\zeta(u)\simeq u$ around 0 for the first integration and $\zeta(u)\simeq(u+1)^2-1$ around -1 for the second integration, T_N can be approximated as

$$T_N\simeq\sqrt{\frac{\pi\eta^2}{N}}\exp\left(\frac{N}{\eta^2}\right). \tag{A9}$$

[1] T. Biancalani, L. Dyson, and A. J. McKane, Noise-Induced Bistable States and Their Mean Switching Time in Foraging Colonies, Phys. Rev. Lett. **112**, 038101 (2014).

[2] O. Feinerman, I. Pinkoviezky, A. Gelblum, E. Fonio, and N. S. Gov, The physics of cooperative transport in groups of ants, Nat. Phys. **14**, 683 (2018).

[3] J. Buhl, D. J. T. Sumpter, I. D. Couzin, J. J. Hale, E. Despland, E. R. Miller, and S. J. Simpson, From disorder to order in marching locusts, Science **312**, 1402 (2006).

[4] I. D. Couzin, J. Krause, N. R. Franks, and S. A. Levin, Effective leadership and decision-making in animal groups on the move, Nature (London) **433**, 513 (2005).

[5] A. Filella, F. Nadal, C. Sire, E. Kanso, and C. Eloy, Model of Collective Fish Behavior with Hydrodynamic Interactions, Phys. Rev. Lett. **120**, 198101 (2018).

[6] C. C. Ioannou, V. Guttal, and I. D. Couzin, Predatory fish select for coordinated collective motion in virtual prey, Science **337**, 1212 (2012).

[7] J. Jhawar, R. G. Morris, U. R. Amith-Kumar, M. Danny Raj, T. Rogers, H. Rajendran, and V. Guttal, Noise-induced schooling of fish, Nat. Phys. **16**, 488 (2020).

[8] R. P. Mann, A. Perna, D. Strömbom, R. Garnett, J. E. Herbert-Read, D. J. T. Sumpter, and A. J. W. Ward, Multi-scale inference of interaction rules in animal groups using Bayesian model selection, PLoS Comput. Biol. **9**, e1002961 (2013).

[9] F. Cucker and S. Smale, Emergent behavior in flocks, IEEE Trans. Automat. Contr. **52**, 852 (2007).

[10] A. Deblais, T. Barois, T. Guerin, P.-H. Delville, R. Vaudaine, J. S. Lintuvuori, J.-F. Boudet, J.-C. Baret, and H. Kellay, Boundaries Control Collective Dynamics of Inertial Self-Propelled Robots, Phys. Rev. Lett. **120**, 188002 (2018).

[11] A. Jadbabaie, J. Lin, and A. S. Morse, Coordination of groups of mobile autonomous agents using nearest neighbor rules, IEEE Trans. Automat. Contr. **48**, 988 (2003).

[12] Shuguang Li, R. Batra, D. Brown, H.-D. Chang, N. Ranganathan, C. Hoberman, D. Rus, and H. Lipson, Particle robotics based on statistical mechanics of loosely coupled components, Nature (London) **567**, 361 (2019).

[13] J. M. Brewer and P. Tsiotras, Partial attitude synchronization for networks of underactuated spacecraft, Automatica **97**, 27 (2018).

[14] R. Bastien and P. Romanczuk, A model of collective behavior based purely on vision, Sci. Adv. **6**, eaay0792 (2020).

[15] C. Bechinger, R. Di Leonardo, H. Löwen, C. Reichhardt, G. Volpe, and G. Volpe, Active particles in complex and crowded environments, Rev. Mod. Phys. **88**, 045006 (2016).

[16] L. Caprini, U. Marconi, and A. Puglisi, Spontaneous Velocity Alignment in Motility-Induced Phase Separation, Phys. Rev. Lett. **124**, 078001 (2020).

[17] S. Chandra, M. Girvan, and E. Ott, Continuous Versus Discontinuous Transitions in the *D*-Dimensional Generalized Kuramoto Model: Odd *D* is Different, Phys. Rev. X **9**, 011002 (2019).

[18] C. Chen, S. Liu, Xia-qing Shi, H. Chaté, and Yilin Wu, Weak synchronization and large-scale collective oscillation in dense bacterial suspensions, Nature (London) **542**, 210 (2017).

[19] H. Ling, G. E. Mclvor, J. Westley, K. van der Vaart, R. T. Vaughan, A. Thornton, and N. T. Ouellette, Behavioural plasticity and the transition to order in jackdaw flocks, Nat. Commun. **10**, 5174 (2019).

[20] C. W. Lynn, L. Papadopoulos, D. D. Lee, and D. S. Bassett, Surges of Collective Human Activity Emerge from Simple Pairwise Correlations, Phys. Rev. X **9**, 011022 (2019).

[21] M. Carmen Miguel, J. T. Parley, and R. Pastor-Satorras, Effects of Heterogeneous Social Interactions on Flocking Dynamics, Phys. Rev. Lett. **120**, 068303 (2018).

[22] K. P. O'Keeffe, H. Hong, and S. H. Strogatz, Oscillators that sync and swarm, Nat. Commun. **8**, 1504 (2017).

[23] H. Shirado and N. A. Christakis, Locally noisy autonomous agents improve global human coordination in network experiments, Nature (London) **545**, 370 (2017).

[24] T. Vicsek and A. Zafeiris, Collective motion, Phys. Rep. **517**, 71 (2012).

[25] A. Hastings, K. C. Abbott, K. Cuddington, T. Francis, G. Gellner, Y.-C. Lai, A. Morozov, S. Petrovskii, K. Scranton, and M. L. Zeeman, Transient phenomena in ecology, Science **361**, eaat6412 (2018).

[26] T. Vicsek, A. Czirók, E. Ben-Jacob, I. Cohen, and O. Shochet, Novel Type of Phase Transition in a System of Self-Driven Particles, Phys. Rev. Lett. **75**, 1226 (1995).

[27] A. Be'er, B. Ilkanaiv, R. Gross, D. B. Kearns, S. Heidenreich, M. Bär, and G. Ariel, A phase diagram for bacterial swarming, Commun. Phys. **3**, 66 (2020).

[28] M. Nagy, G. Vásárhelyi, B. Pettit, I. Roberts-Mariani, T. Vicsek, and D. Biro, Context-dependent hierarchies in pigeons, Proc. Natl. Acad. Sci. USA **110**, 13049 (2013).

[29] A. Attanasi, A. Cavagna, L. Del Castello, I. Giardina, T. S. Grigera, A. Jelić, S. Melillo, L. Parisi, O. Pohl, E. Shen *et al.*, Information transfer and behavioural inertia in starling flocks, Nat. Phys. **10**, 691 (2014).

[30] C. Escudero, C. A. Yates, J. Buhl, I. D. Couzin, R. Erban, I. G. Kevrekidis, and P. K. Maini, Ergodic directional switching in mobile insect groups, Phys. Rev. E **82**, 011926 (2010).

[31] C. A. Yates, R. Erban, C. Escudero, I. D. Couzin, J. Buhl, I. G. Kevrekidis, P. K. Maini, and D. J. T. Sumpter, Inherent noise can facilitate coherence in collective swarm motion, Proc. Natl. Acad. Sci. USA **106**, 5464 (2009).

[32] R. Piwowarczyk, M. Selin, T. Ihle, and G. Volpe, Influence of sensorial delay on clustering and swarming, Phys. Rev. E **100**, 012607 (2019).

[33] Y. Sun, W. Lin, and R. Erban, Time delay can facilitate coherence in self-driven interacting-particle systems, Phys. Rev. E **90**, 062708 (2014).

[34] R. Erban, J. Haskovec, and Y. Sun, A Cucker–Smale model with noise and delay, SIAM J. Appl. Math. **76**, 1535 (2016).

[35] M. Mijalkov, A. McDaniel, J. Wehr, and G. Volpe, Engineering Sensorial Delay to Control Phototaxis and Emergent Collective Behaviors, Phys. Rev. X **6**, 011008 (2016).

[36] R. Olfati-Saber and R. M. Murray, Consensus problems in networks of agents with switching topology and time-delays, IEEE Trans. Automat. Contr. **49**, 1520 (2004).

[37] P. E. Kloeden and E. Platen, Stochastic differential equations, in *Numerical Solution of Stochastic Differential Equations* (Springer, New York, 1992), pp. 103–160.

[38] T. D. Frank, Delay Fokker-Planck equations, Novikov's theorem, and Boltzmann distributions as small delay approximations, Phys. Rev. E **72**, 011112 (2005).

[39] C. W. Gardiner *et al.*, *Handbook of Stochastic Methods*, Vol. 3 (Springer, Berlin, 1985).

[40] Y. Guo, W. Lin, and G. Chen, Stability of switched systems on randomly switching durations with random interaction matrices, IEEE Trans. Automat. Contr. **63**, 21 (2018).

[41] S. Zhou, Y. Guo, M. Liu, Y.-C. Lai, and W. Lin, Random temporal connections promote network synchronization, Phys. Rev. E **100**, 032302 (2019).

[42] J.-W. Hou, H.-F. Ma, D. He, J. Sun, Q. Nie, and W. Lin, Harvesting random embedding for high-frequency change-point detection in temporal complex systems, Nat. Sci. Rev. **9**, nwab228 (2022).

[43] S. Leng, H. Ma, J. Kurths, Y.-C. Lai, W. Lin, K. Aihara, and L. Chen, Partial cross mapping eliminates indirect causal influences, Nat. Commun. **11**, 2632 (2020).

[44] X. Ying, S.-Y. Leng, H.-F. Ma, Q. Nie, Y.-C. Lai, and W. Lin, Continuity scaling: A rigorous framework for detecting and quantifying causality accurately, Research **2022**, 9870149 (2022).

[45] P. S. Skardal and A. Arenas, Higher order interactions in complex networks of phase oscillators promote abrupt synchronization switching, Commun. Phys. **3**, 218 (2020).

[46] J. E. Herbert-Read, A. Perna, R. P. Mann, T. M. Schaerf, D. J. T. Sumpter, and A. J. W. Ward, Inferring the rules of interaction of shoaling fish, Proc. Natl. Acad. Sci. USA **108**, 18726 (2011).

[47] S. B. Rosenthal, C. R. Twomey, A. T. Hartnett, H. S. Wu, and I. D. Couzin, Revealing the hidden networks of interaction in mobile animal groups allows prediction of complex behavioral contagion, Proc. Natl. Acad. Sci. USA **112**, 4690 (2015).

[48] C. Huepe, G. Zschaler, Anne-Ly Do, and T. Gross, Adaptive-network models of swarm dynamics, New J. Phys. **13**, 073022 (2011).